Polymer Chemistry

Accepted Manuscript

ROYAL SOCIETY OF CHEMISTRY

www.rsc.org/polymers

Polymer Chemistry

RSCPublishing

ARTICLE

Electrochemical Deposition of Polypeptides: Bio-based Covering Materials for Surface Design†

Cite this: DOI: 10.1039/xoxxoooooox

Huseyin Akbulut,[a] Murat Yavuz,[b,c] Emine Guler,[b] Dilek Odaci Demirkol,[b] Takeshi Endo,[*d] Shuhei Yamada,[d] Suna Timur*[b] and Yusuf Yagci*[a]

Received ooth January 2014,
Accepted ooth January 2014

DOI: 10.1039/xoxxoooooox

www.rsc.org/

A simple and efficient approach for the electrochemical deposition of polypeptides as bio-based covering materials for surface design is described. The method involves *N*-carboxyanhydride (NCA) ring-opening polymerization from its precursor to form a thiophene-functionalized polypeptide macromonomer (T-Pala), followed by electropolymerization. The obtained conducting polymer, namely polythiophene-g-polyalanine (PT-Pala), was characterized and utilized as a matrix for biomolecule attachment. The biosensing applicability of PT-Pala was also investigated by using glucose oxidase (GOx) as a model enzyme to detect glucose. The designed biosensor showed a very good linearity for 0.01–1.0 mM glucose. Finally, the antimicrobial activities of newly synthesized T-Pala and PT-Pala were also evaluated by the disc diffusion method.

Introduction

Innovative approaches for the syntheses of polymeric structures bearing polypeptides have received enormous interest in the fields of biomedicine, drug delivery, biomineralization, nanoscale self-assembly, and tissue engineering. The conjugation of synthetic polymers with polypeptides can result in novel biomaterials that possess the following characteristics: biorecognition-like properties similar to antibody/antigen interactions, biodegradability properties, biocatalyst activity, and compatibility with blood and/or tissue.[1-5] Polypeptides, showing three-dimensional conformations such as α-helix, β-sheet, and random coil structures, could exhibit intriguing self-assembling behavior. Due to these unique features, they impart interesting properties and functions to any polymeric structure in which they are combined.[6,7] Traditionally, most peptides have been prepared[8] by the ring-opening polymerization of the corresponding α-amino acids of *N*-carboxyanhydrides (NCAs).

Generally, primary and secondary amines most favorably initiate NCA polymerization. Their "living" nature allows the decisive control of a certain molecular weight and terminal structure.[7,9] Although the "living" polymerization of NCA is a significant challenge in the synthesis of polypeptides based on natural or unnatural amino acids, the polymerization reaction requires extreme impurity-free conditions to achieve the polymerization without side reactions. Thus, extensive research worldwide has aimed at developing new methods for reliable syntheses of monomers that are appropriate for NCA polymerization. However, earlier attempts[10-16] for NCA synthesis either involve multistep reactions or the use of hazardous reagents such as phosgene, or they lack sufficient monomer purity for the polymerization. Moreover, the vulnerable nature of NCA in the presence of water contamination or under heating conditions is the main drawback, requiring the reaction to proceed under impractical conditions.[4,9] Thus, research has been devoted to obtain NCAs from nontoxic materials with high purity and stability though the development of new synthetic strategies.

In related studies carried out the laboratory of one of the authors of this paper, different NCAs were obtained via intramolecular cyclization of activated urethane derivatives of α-amino acids by a simple procedure.[9,17-20] The method offers a practical and green way for polypeptide synthesis without the use and production of any toxic compounds. Quite recently, the method was further improved by taking advantage of consecutive NCA formation and polymerization processes.[9] Thus, the precursor urethane derivatives were readily synthesized by a two-step procedure: (i) transformation of α-amino acids into the corresponding ammonium salts and (ii) *N*-carbamylation of the salts with diphenyl carbonates. These compounds are stable at room temperature for months and can be converted into polypeptides simply by heating in dimethyl acetamide (DMAc) in the presence of primary amines through *in situ* NCA formation and polycondensation with the elimination of phenol and CO_2.

Conjugated polymers, in particular those based on thiophene and its derivatives, have been extensively studied because of their applicability in the fabrication of electronics and electro-optic devices due to their characteristic electronic and optical properties.[21] These polymers have been synthesized by various coupling reactions as well as oxidative and electropolymerization

processes, which provide films with different morphologies and, consequently, different physical and chemical properties.[22] Previously, it has been shown that polythiophenes (PTs) can be combined with conventional synthetic polymers through the combination of various chain polymerization processes with electropolymerization.[23-33] However, the corresponding conjugation of PT with biomolecules has been rarely investigated.[34-38] Reported examples involve a postmodification approach on the surface of PT films. For example, PT containing highly reactive *p*-benzenesulfonyl chloride groups was prepared by electropolymerization, and subsequent covalent protein immobilization was achieved by a nucleophilic reaction.[34] In another study, a peptide-modified PT biosensor was developed for electrochemical analysis of copper ions. The tripeptide Gly–Gly–His, which selectively recognizes copper ions, was covalently immobilized to the PT film.[34] In addition, besides covalent immobilization,[36,37] π-π stacking interactions have been successfully used for the postmodification of PTs and other conjugated polymers.[38]

Taking into consideration all of the above-mentioned views, herein we report the synthesis, characterization, and biosensing application of PT bearing polyalanine homopeptide side chains (PT-Pala). This complex macromolecular architecture was prepared directly by NCA ring-opening polymerization reactions from its precursor to form the polypeptide macromonomer, followed by electropolymerization. To the best of our knowledge, no such conjugated graft copolymer with a variety of potential biological applications has been reported previously. As presented below, this combination has led to promising results in terms of biosensor and bioconjugation applications by taking advantage of the fluorescence features and reactivity of the amino side chains of PT and the polypeptide, respectively. Glucose oxidase (GOx) was used as a model enzyme, and immobilization of the biocomponent was carried out using glutaraldehyde, which forms a covalent bond between electrodeposited PT-Pala and the biomolecule through the amino groups of the polypeptide. The applicability of PT-Pala film as an immobilization matrix was investigated by monitoring the electrochemical biosensor responses using glucose as the substrate. The surface features of the film were examined by Fourier transform infrared (FTIR) spectroscopy, scanning electron microscopy (SEM), and fluorescence microscopy. In addition, electrochemical characterization of the PT-Pala-coated electrodes was performed. Finally, the antimicrobial activities of the newly synthesized thiophene-polyalanine macromonomer (T-Pala) and polymer (PT-Pala) were evaluated by using the disc diffusion method.

Results and discussion

Electroactive polypeptide macromonomer

The possibility of NCA ring-opening polymerization with primary amines and electropolymerization of thiophene and its derivatives prompted us to combine these systems for the synthesis of PT-based graft copolymers with polypeptide side chains. Accordingly, graft copolymers were obtained in two discrete steps. In the first step, the polypeptide macromonomer T-Pala was synthesized via the ring-opening polymerization of L-Ala-*N*-(phenyloxycarbonyl)amino acid with an amino initiator. As the thiophene polypeptide macromonomer was intended to be used in a further electropolymerization reaction, the synthetic strategy for the functional primary amino initiator was selected so as to preserve the 2- and 5-positions of the thiophene ring. Thus, 3-(aminomethyl)thiophene was readily synthesized according to the following reactions in high yields (Fig. 1).

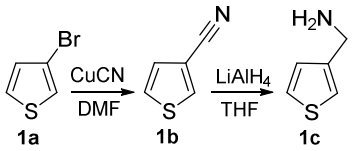

Fig. 1 Preparation of 3-(aminomethyl)thiophene (1c) as the initiator of NCA polymerization.

The NCA precursor, L-Ala-*N*-(phenyloxycarbonyl) amino acid, i.e., the urethane derivative of an α-amino acid, was synthesized by successive protection of the acid group of alanine (**2a**) by an ionic exchange reaction with the corresponding ammonium salt and *N*-carbamylation of the ammonium salt-protected amino acid (**2b**) via the nucleophilic attack of the active primary amino group of **2b** toward the carbonyl group of diphenyl carbonate (DPC) (Fig. 2).

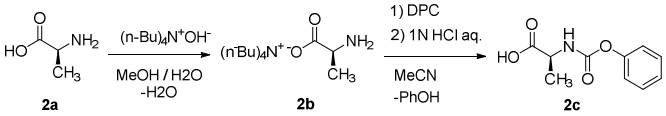

Fig. 2 Synthetic route towards L-Ala-*N*-(phenyloxycarbonyl)amino acid (2c).

Polymerization of the NCA precursor (**2c**) proceeded in the presence of DMAc and **1c** as the solvent and initiator, respectively, in a one-pot reaction through *in situ* intramolecular cyclization followed by a ring-opening reaction with CO_2 elimination (Fig. 3).

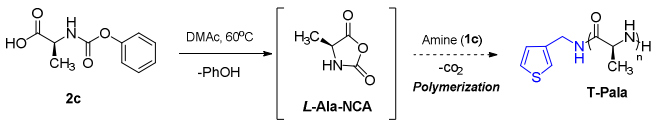

Fig 3 Synthesis of thiophene-polyalanine (T-Pala).

This strategy directly afforded the formation of NCA in the polymerization media and eliminated problems associated with the monomer purity and stability. The conditions of polymerization, i.e., a high concentration of the initiator with respect to the monomer, were chosen to obtain a low molecular weight polymer (M_n = 1140 g mol^{-1}), combined with a satisfactory conversion (80% yield) and polydispersity (M_w/M_n = 1.16) suitable for the subsequent electropolymerization process. Although the polyalanine chain has minimal steric hindrance among all types of polypeptides, high molecular weight polymers have low solubility in any solvent.

The structure of T-Pala was investigated by proton nuclear magnetic resonance (^{1}H-NMR) and Fourier transform infrared (FTIR) spectroscopy. In the ^{1}H-NMR spectrum of T-Pala, broad

bands at 4.30–4.48 ppm and 1.45–1.65 ppm corresponding to –CH and –NH groups of the repeating unit indicate the polymeric structure. The terminal thiophene groups were confirmed by a doublet at 3.48 ppm, a doublet at 7.00 ppm, and singlets at 7.05 and 7.46 ppm. The $–NH_2$ terminal group resonates at 7.68–7.74 ppm.

Electrodeposition of T-Pala and enzyme immobilization

PT-Pala film formation was performed via electrochemical polymerization at a potential of +1.6 V vs. Ag/AgCl. The charge and the thickness of the electrodeposited PT-Pala film were calculated as 248.8 mC and 5.53 µm, respectively. Afterwards, it was used as a functional platform containing the peptide handles on the surface for biomolecule immobilization. GOx was used as a model enzyme and was immobilized on the amino termini of the peptide chains on each thiophene unit by means of glutaraldehyde. Fig. 4 describes each surface modification and the biosensor fabrication steps.

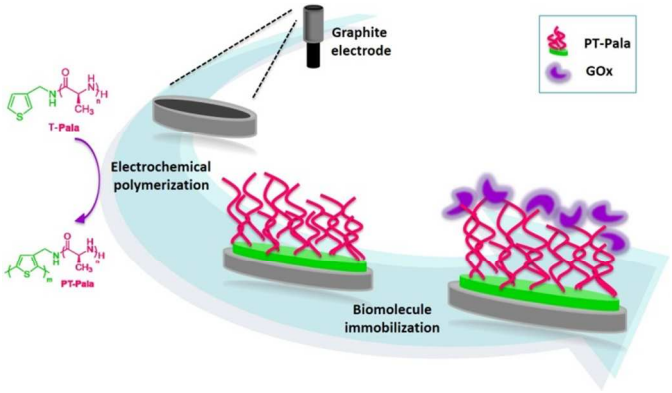

Fig. 4 Schematic representation of PT-Pala film formation and construction of the PT-Pala film/GOx biosensor.

Characterization of the PT-Pala film

Both T-Pala and PT-Pala were characterized by FTIR spectral analysis. In the FTIR spectrum of the monomer, the following absorption peaks were identified: 3266 cm^{-1} and 3074 cm^{-1} (N–H vibration), 2978 cm^{-1} and 2874 cm^{-1} (aliphatic methylene stretching vibration), 1624 cm^{-1} (C=O stretching vibration), and 1222 cm^{-1} (C–C stretching vibration arising from a carbonyl group bonded to an alkyl group). The absorption bands at 1532, 778, and 698 cm^{-1} were due to the vibrations of C–H and C=C bonds of thiophene rings. The FTIR spectrum of the polymer revealed that electropolymerization of T-Pala was successfully achieved on the surface of the graphite electrode. The peak monitored at 778 cm^{-1} indicated cis C–H wagging of the thiophene ring, and the band at 698 cm^{-1} due to deformations of C–H out of the plane of the thiophene ring disappeared completely upon polymerization. In addition, new absorption bands became pronounced at 760 cm^{-1} (thienylene C–Hα tri-substituted ring bend) and 1002 cm^{-1} (thienylene C–Hα in-plane bend). The strong peak observed at 1192 cm^{-1} (S=O stretching vibration of SO_3^-) was characteristic of the sodium dodecyl sulfate (SDS) dopant ion peak. The medium and broad peak monitored at 1682 cm^{-1} was the C=O stretching vibration arising from the carbonyl group. The intensity of that peak was relatively low when compared to the intensity of the carbonyl peak of the monomer (ESI, Fig. S1†). It should also be pointed out that the obtained polymer is expected to have a copolymer structure rather than composite consisting of independent polymer chains. In the electrocopolymerization of such monomer and macromonomer couples, chemical linking of the segments occurs through the coupling reaction at 2 and 5, and unsubstituted 3 and 4 poisitons of the thiophene ring[23-33].

Cyclic voltammetry (CV) was used to investigate the electron transfer process on the biofilm surface. As well as CV of bare graphite, PT-Pala- and PT-Pala/GOx-modified graphite electrodes were obtained in a mixture of 5.0 mM $Fe(CN)_6^{3-/4-}$ and 0.1 M KCl. As shown in Fig. 5, the PT-Pala-modified graphite electrode had greater peak currents (38.514 µA, ΔE_{Pc} = 0.278 V) than the bare electrode (16.289 µA, ΔE_{Pc} = 0.268 V). This result is related to the enhanced conductivity of the polymer film, which is important for biosensor response and can be attributed to the increased number of functional amino groups caused by electrodeposited peptides. Thus, negatively charged $Fe(CN)_6^{3-/4-}$ is attracted to the electrode surface. After biomolecule immobilization, the peak current (24.362 µA, ΔE_{Pc} = 0.296 V) decreased in comparison with the PT-Pala-coated graphite electrode. This result was expected due to the modification of the electrode surface with the biomolecule, which diminished the electron transfer properties because of a possible diffusion layer. The obtained results clearly confirm that the immobilization steps for biosensor fabrication were carried out successfully.

Furthermore, cyclic voltammograms of PT-Pala- and PT-Pala/GOx-modified electrodes at different scan rates are shown in the Fig. S2A–B of ESI† section. For PT-Pala-coated graphite, the square root of the scan rate-dependent anodic and cathodic linear equations are defined by y = -6.232x - 3.763 (R^2 = 0.992) and y = 4.336x + 6.103 (R^2 = 0.981), respectively. In the case of PT-Pala/GOx-modified graphite, the linearity of the anodic and cathodic signals is defined by the following equations: y = -4.634x + 0.061 (R^2 = 0.996) and y = 2.322x + 5.423 (R^2 = 0.972), respectively. Both the anodic and cathodic peak currents were linearly proportional to the square root of the scan rate, in the range from 5.0 to 200 mV/s (ESI, Fig. S2A–B† (inset)), indicating a diffusion-controlled electrode process.

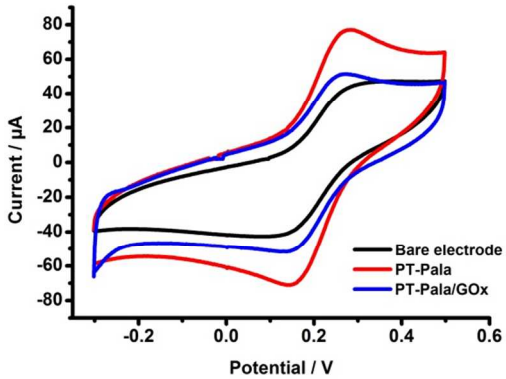

Fig. 5 CVs of the bare graphite electrode, PT-Pala-coated electrode, and GOx-immobilized PT-Pala-coated electrode (in 5.0 mM $Fe(CN)_6^{3-/4-}$, at a scan rate of 50 mV s^{-1}).

Surface characterization

The surface morphology of the PT-Pala film was monitored by SEM and compared with those of the electrodeposited PT and PT-Pala/PT copolymers. In the case of PT, granular morphology was observed; however, PT-Pala showed a completely different surface morphology. A homogeneous film was observed on the graphite surface; but when both PT and the PT-Pala/PT copolymer were used for the electrodeposition, a mixed structure of both PT and PT-Pala was obtained as shown in Fig. 6.

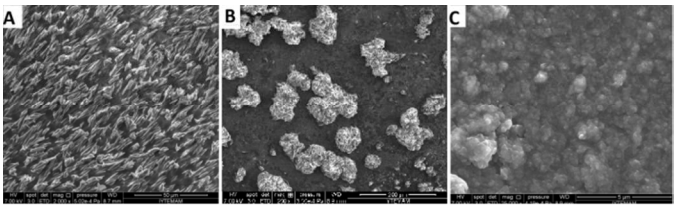

Fig. 6 SEM images of (A) PT-Pala-, (B) PT-Pala/PT-, and (C) PT-coated electrodes.

T-Pala deposition on indium tin oxide coated glass was also observed by fluorescence microscopy after formation (ESI, Fig. S3†). The polymer matrix can be seen clearly because of the fluorescent characteristic of the PT-Pala film.

Biosensing applications

The effect of pH on the sensitivity of the PT-Pala/GOx biosensor was optimized using 1.0 mM glucose as the substrate. The pH of acetate buffer was varied from pH 3.5 to pH 5.5. The relative biosensor response (%) was plotted against different pH values. According to Fig. S4 (ESI†), the maximum activity was at pH 4.5, which is close to the optimum pH for free GOx.

Afterwards, chronoamperometric responses of the biosensor were recorded by adding standard solutions of glucose to reaction buffer solution. Fig. 7 shows the calibration curve for glucose (the inset shows the linear range of the calibration curve). There was a linear relationship between the obtained current and the glucose concentration in the concentration range of 0.01–1.0 mM. To test repeatability, the biosensor signals corresponding to 0.5 mM glucose solutions were measured. The standard deviation and variation coefficient (%) were calculated to be ±0.016 and 3.25%, respectively.

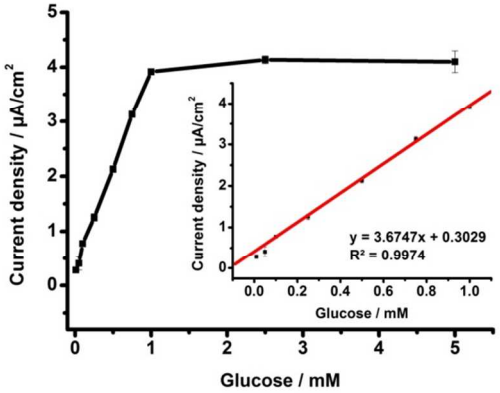

Fig. 7 Calibration curve for glucose. PT-Pala/GOx in 50 mM sodium acetate, pH 4.5, 25 °C, −0.7 V. Error bars show the standard deviation of three measurements (the inset shows the linear range).

In addition, calibration curves were also plotted using PT- and PT-Pala/PT copolymer-coated graphite electrodes for the construction of GOx biosensors under identical experimental conditions. Insignificant response signals were obtained in a narrower linear range of glucose (0.01–0.8 mM) with a longer response time in comparison to the PT-Pala/GOx electrode.

To observe the effect of covalent immobilization on the current responses, another biosensor was prepared by the physical adsorption. In this case, the enzyme electrode was constructed without using glutaraldehyde and a calibration graph was plotted to compare the response characteristics with the GOx electrode obtained by the covalent immobilization procedure (ESI, Fig. S5†). The linearity was obtained from 0.05 to 1.0 mM for glucose, with the equation of y=2.415x+ 0.366, (R^2:0.989). Moreover, the biosensing performance was tested by successively measuring of the responses by the addition of glucose (0.5 mM). The variation coefficient was calculated as 16.12%. The results showed that the biosensor constructed by the physical adsorption exhibited the lower sensitivity (as can be seen from the slopes of the linear plots) and un-acceptable RSD value which shows non-repetitive signals. It could be explained by the weak interactions between the biomolecule and the surface as a result of a short incubation time (90 min). Thus, the leakage of the biomolecules from the surface was occurred easily and it caused un-reproducible response signals after each trial. On the other side, these findings show that the polymer matrix could have a potential for the biomolecule adsorption, but in that case, longer incubation times in the immobilization procedures, are required. Also, the adsorption time as well as the enzyme amount should be optimized as the important parameters to have more reproducible and reliable response signals.

In addition to covalent immobilization, there are different immobilization techniques including adsorption, entrapment, cross-linking which present different advantages and drawbacks. Among these techniques, covalent immobilization depending on the formation of chemical bonds between functional groups of the enzyme and the matrix has some advantages such as stable and compact structure, short response time and no diffusion barrier.[39] Table 1 presents a comparison of some glucose biosensors constructed using different immobilization techniques that were reported in literature.

Table 1. Comparison of some glucose biosensors constructed with different immobilization techniques, in terms of linearity and the relative standard deviation (RSD) in the literature.

Electrode	Immobilization method	Linear range (mM)	RSD (%)	Reference
SPCE	Adsorption	0.2–7.5	ND	40
GCE	Adsorption	0.05-10.50	ND	41
GCE	Adsorption	0.1–5.0	3.79	42
PDE	Adsorption	0.2-9.1	3.6	43
Fe working electrode	Entrapment	0.025-3.0	3.5	44
CNT paste electrode	Entrapment	Up to 0.8	ND	45
Au electrode	Crosslinking	0.05-12	2.2	46
BDD electrode	Crosslinking	0-25	ND	47
GCE	Affinity	1.8×10^{-3}-5.15	2.5	48
Pt microelectrode	Affinity	Up to 2.4	ND	49

GE	Covalent immobilization	0.02-1.20	ND	50
GE	Covalent immobilization	0.025-1.25	5.87	51
GE	Covalent immobilization	0.01–1.0	3.25	This work

SPCE: The screen-printed carbon electrode, GCE: Glassy carbon electrode, CNT: Carbon nanotube, PDE: Platinum disk electrode, BDD: Boron-doped diamond, Pt: Platinum, GE: Graphite electrode, ND: Not detected.

Also, antimicrobial activities of the novel thiophene-polyalanine macromonomer (T-Pala) and polymer (PT-Pala) were evaluated by using the disc diffusion method (ESI, Table S1 and Fig. S6†). The results showed that PT-Pala exhibited moderate antibacterial activity towards Gram-positive bacteria. Graphite covered with PT-Pala also showed significant antibacterial activity against Gram-positive *S. aureus* ATCC 25923.

Experimental section

Materials

3-Bromothiophene, copper (I) cyanide, lithium aluminium hydride, L-alanine, tetrabuthylammonium hydroxide, and diphenyl carbonate were purchased from Sigma-Aldrich and were used as received. DMAc and DMF were purified by heating at 60 °C for 1 h over calcium hydride (CaH_2), followed by fractional distillation before use.

Synthesis of thiophene-3-carbonitrile (1b). 3-Bromothiophene (**1a**; 1.63 g, 10 mmol) and CuCN (3.58 g, 40 mmol) dissolved in 15 mL of DMF were placed in a Schlenk tube under a nitrogen atmosphere, and the mixture was stirred at 150 °C for 18 h. Then, the temperature was allowed to drop to room temperature and 40 mL of 14% NaOH was added to the mixture. Next, 300 mL of diethyl ether was added to the aqueous phase, and the mixture was vigorously stirred at room temperature for 30 min. Afterwards, the organic layer was washed with water and dried over $NaSO_4$. After evaporation of the solvent until near dryness, the residue was purified by flash chromatography (silica gel, 1:1 chloroform-hexane as the eluent) to provide 765 mg of product in ~70% overall yield. ^{1}H-NMR ($CDCl_3$, 500 MHz): δ 7.89 (s, 1H), 7.38 (d, 1H), 7.18 (d, 1H).

Synthesis of 3-(aminomethyl)thiophene (1c). To a solution of lithium aluminum hydride (417 mg, 11 mmol) in 15 mL of dry THF at 0 °C, thiophene-3-carbonitrile (**1b**; 1.0 g, 9.16 mmol) in 15 mL of dry THF was added over 20 min under a nitrogen atmosphere, and the mixture was warmed to 50 °C over 2 h. The reaction mixture was cooled to 0 °C, and 2.0 mL of 15% NaOH was added dropwise before 6.0 mL of water was added to the mixture. The aqueous layer was extracted with diethyl ether (50 mL × 5). Then, the organic layer was concentrated by evaporation. The oily residue was purified by fractional distillation under vacuum to give 870 mg of product as a colorless oil in ~70% overall yield. ^{1}H-NMR ($CDCl_3$, 500 MHz): δ 7.31 (d, 1H), 7.15 (s, 1H), 7.03 (d, 1H), 3.90 (s, 2H), 1.47 (s, 2H).

Synthesis of L-Ala-*N*-(phenyloxycarbonyl) amino acid. To a stirred solution of L-alanine (1.78 g, 20 mmol) in methanol (30 mL), tetrabutylammonium hydroxide (37% in methanol, 13.8 g, 20 mmol) was slowly added at room temperature. After stirring for 1 h, the reaction mixture was concentrated under reduced pressure. The resulting residue was dissolved in acetonitrile (20 mL). The solution was added dropwise over 10 min to a stirred solution of DPC (4.2 g, 20 mmol) in acetonitrile (25 mL) under ambient conditions, and then the reaction mixture was stirred for 3 h. To the reaction mixture, 1.0 M HCl aqueous solution (20 mL) was added. The mixture was transferred into a separatory funnel containing distilled water (30 mL), and the organic fractions were combined, washed with brine, dried over Na_2SO_4, filtered, and concentrated under reduced pressure. The crude products were purified by flash column chromatography with a gradient from 50–70% ethyl acetate in *n*-hexane as the eluent, followed by recrystallization with ethyl acetate/*n*-hexane to yield 2.5 g of product as a white powder in 60% yield. ^{1}H-NMR ($CDCl_3$, 500 MHz): δ 1.55 (d, J = 7.2 Hz, 3H), 4.49 (dt, J = 14.0, 6.9 Hz, 1H), 5.60 (d, J = 7.1 Hz, 1H), 7.14 (d, J = 7.9 Hz, 2H), 7.21 (t, J = 7.4 Hz, 1H), 7.36 (t, J = 7.8 Hz, 2H).

Synthesis of T-Pala in the presence of 3-(aminomethyl)thiophene. L-Ala-*N*-(phenyloxycarbonyl)amino acid (**2c**) (206 mg, 1.0 mmol) dissolved in 1.0 mL of dry DMAc and 3-(aminomethyl)thiophene (**1c**)/DMAc solution (20 μL, 1.0 × 10^{-2} mmol/μL) was placed into a flame-dried Schlenk tube. The polymerization was carried out at 60 °C for 48 h under a nitrogen atmosphere. Next, the reaction mixture was cooled to room temperature, and the white blurry solid was poured into diethyl ether and stirred for 2 h at room temperature to eliminate unreacted monomer and other contaminants. The white precipitates were collected by filtration and dried under vacuum to yield 73 mg of T-Pala in 80% yield. *Mn*: 1140, M_w/Mn = 1.16. ^{1}H-NMR ($CDCl_3$, 500 MHz): δ 1.45-1.65 (br, 3H), 3.45-3.52 (br, 2H), 4.10-4.25 (br,1H), 4.27-4.52 (br, 3H), 6.98-7.30 (br, 1H), 7.13-7.15 (br, 1H), 7.27-7.30 (br, 1H).

Preparation of PT, PT-Pala, and PT-Pala/PT biosensors

Initially, spectroscopic grade graphite electrodes were polished on emery paper and washed thoroughly with distilled water to be used in the polymerization reaction. In order to achieve electrochemical polymerization, T-Pala was initially subjected to chronoamperometry by applying +1.6 V in 0.1 M SDS in 30:70 water/acetonitrile solutions for 20 min. The reaction pathway is illustrated in Fig. 8. For electrochemical copolymerization of T-Pala/thiophene, 0.1 M thiophene was added to the solution and the same reaction conditions were applied. In the case of bare PT matrix, 0.1 M thiophene, 0.1 M SDS, and 10 mL of distilled water were used and +1.6 V was applied.

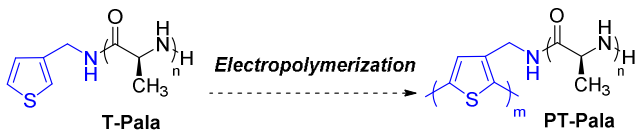

Fig. 8 Synthesis of the PT-Pala electropolymer.

For enzyme immobilization, a proper amount of GOx (1.0 mg in 5.0 μL, 50 mM sodium phosphate buffer, pH 7.0) was spread over the polymer-coated electrodes, glutaraldehyde (5.0 μL, 0.1% in

50 mM sodium phosphate buffer, pH 7.0) was added, and the electrodes were allowed to stand at ambient conditions to dry for 90 min. To confirm the efficiency of the covalent immobilization to biosensor response, a control experiment in the absence of glutaraldehyde under identical experimental conditions was also performed.

Measurements

^{1}H-NMR spectra were recorded with an Agilent VNMRS 500 MHz, and chemical shifts were recorded in ppm units using tetramethylsilane as an internal standard. For amperometric measurements, the radiometer electrochemical measurement unit (VoltaLab PGP201, Lyon, France) was used with a traditional three-electrode configuration. A graphite electrode (Ringsdorff Werke GmbH, Bonn, Germany, type RW001, 3.05-mm diameter and 13% porosity) as the electrode for biomolecule attachment, a Ag/AgCl electrode as the reference electrode, and a platinum electrode as the counter electrode were used during electrochemical measurements, and all potentials were reported with respect to the Ag/AgCl reference electrode. A Palm Instruments potentiostat (PalmSens, Houten, The Netherlands, www.palmsens.com) with three electrode configurations was used for the CV experiments. FTIR-attenuated total reflection (ATR) spectra were recorded in the wavenumber range from 4000–650 cm^{-1} with a Spectrum BX-II Model instrument (Perkin Elmer, Norwalk, CT, USA) and an attached MIRacle ATR diamond crystal unit (Pike Technologies, Madison, WI, USA). A resolution of 4 cm^{-1} and 50 scans per sample were used. An Olympus BX53F Fluorescence microscope with an Olympus DP72 camera and an Uplanapo 100× objective and SEM (FEI QUANTA250 FEG) were used for surface imaging of the prepared electrodes.

For determination of the number average molecular weight (*Mn*) and polydispersity index (*Mw*/*Mn*) for the synthesized polymers, a gel permeation chromatography (GPC) analysis was performed on an Agilent 1100 Series instrument, including a pump, NUCLEOGEL® GPC columns, and a differential refractive index (RI) detector, at a flow rate of 0.7 mL/min using 0.01 M LiBr/DMF as the eluent and 50 °C. Toluene was chosen as the flow marker, and the RI detector was calibrated with poly(methyl methacrylate) standards having a molecular weight of 2.500–270.000 g/mol.

Electrochemical measurements

Amperometric determination of the biosensor response was performed at ambient conditions by applying a constant potential at –0.7 V and following the oxygen consumption as a result of enzymatic activity in the bioactive surface. The enzyme electrodes were initially equilibrated in 10 mL of sodium acetate (pH:4.5) as a working buffer. When the background current reached a steady state, the substrate solution was added to the electrochemical cell, then the current change was monitored as current density ($\mu A/cm^2$), and the steady-state current values were recorded. In all amperometric studies, each measurement was repeated three times, and standard deviations were calculated. All reported data were given as the average of three measurements ± standard deviation. In the figures, error bars show standard deviation. The experiments were conducted at ambient temperature (25 °C).

Antimicrobial activities

Antimicrobial activities of the thiophene-polyalanine macromonomer (T-Pala) and polymer (PT-Pala) were evaluated by using the disc diffusion method (details are given in ESI).

Conclusion

In conclusion, we designed and demonstrated a facile and generally applicable technique for the formation of novel, bio-functional immobilization platform, on graphite for use as a matrix for biomolecule attachment via the ring-opening polymerization of NCA directly from the precursor and subsequent electropolymerization. This technique is experimentally facile and can be applied to various types of polypeptides. In the present work, the concept was successfully tested for the preparation of the functional PT-Pala and subsequent GOx attachment. Further experiments demonstrated the biosensing applicability of the electroactive conjugated polymers. The bio-application of these types of polymers is unprecedented. Moreover, the described strategy is not restricted to the model peptide employed here and can be potentially extended to a very broad range of peptides by using their NCA precursors in the related ring-opening polymerization. Thus, the properties of the side chain polypeptides on the conducting layer can be tuned for various bio-applications, such as cell culture on a chip.

Notes and references

[a] Department of Chemistry, Faculty of Science and Letters, Istanbul Technical University, Istanbul, Turkey.
[b] Department of Biochemistry, Faculty of Science, Ege University, Bornova, 35100, Izmir, Turkey.
[c] Department of Chemistry, Faculty of Science, Dicle University, 21280, Diyarbakir, Turkey.
[d] Molecular Engineering Institute, Kinki University, 11-6 Kayanomori, Iizuka, Fukuoka 820-8555, Japan.
[*] Corresponding authors E-mail : yusuf@itu.edu.tr (Y. Yagci)
sunatimur@yahoo.com (S. Timur)
tendo@moleng.fuk.kindai.ac.jp (T. Endo)

† Electronic Supplementary Information (ESI) available: FT-IR spectra of T-Pala and PT-Pala, characterization and electrochemical behavior of PT-Pala and evaluation of antimicrobial activity were given as supplementary information. See DOI: 10.1039/b000000x/

1 Y. Dai, M. Xu, J. Wei, H. Zhang and Y. Chen, *Appl. Surf. Sci.* 2012, **258**, 2850.
2 M. E. M. Barbosa, V. Montembault, S. Cammas-Marion, G. Ponchel and L. Fontaine, *Polym. Int.* 2007, **56**, 317.
3 J. Ling, H. Peng and Z. Shen, *J. Polym. Sci., Part A-1: Polym. Chem.* 2012, **50**, 3743.

4 G. J. M. Habraken, M. Peeters, C. H. J. T. Dietz, C. E. Koning and A. Heise, *Polym. Chem.* 2010, **1**, 514.
5 R. Obeid and C. Scholz, *Biomacromolecules* 2011, **12**, 3797.
6 K. Ishikawa and T. Endo, *J. Am. Chem. Soc.* 1988**, 110**, 2016.
7 K. Koga, A. Sudo, H. Nishida and T. Endo, *J. Polym. Sci., Part A-1: Polym. Chem.* 2009, **47**, 3839.
8 J. W. Robinson and H. Schlaad, *Chem. Commun.* 2012, **48**, 7835; J. Sun and H. Schlaad, *Macromolecules* 2010, **43**, 4445; K.-S. Krannig and H. Schlaad, *J. Am. Chem. Soc.* 2012, **134**, 18542; T. Aliferis, H. Iatrou and N. Hadjichristidis, *Biomacromolecules* 2004, **5**, 1653; H. Iatrou, H. Frielinghaus, S. Hanski, N. Ferderigos, J. Ruokolainen, O. Ikkala, D. Richter, J. Mays and N. Hadjichristidis, *Biomacromolecules* 2007, **8**, 2173; N. Hadjichristidis, H. Iatrou, M. Pitsikalis and G. Sakellariou, *Chem. Rev.* 2009, **109**, 5528.
9 S. Yamada, K. Koga and T. Endo, *J. Polym. Sci., Part A-1: Polym. Chem.* 2012, **50**, 2527.
10 Y. Fujita, K. Koga, H.-K. Kim, X.-S. Wang, A. Sudo, H. Nishida and T. Endo, *J. Polym. Sci., Part A-1: Polym. Chem.* 2007, **45**, 5365.
11 H. Leuchs, *Ber. Dtsch. Chem. Ges.* 1906, **39**, 857.
12 T. Curtius, K. Hochschwender, H. Meier, W. Lehmann, A. Benckiser, M. Schenck, W. Wirbatz, J. Gaier and W. Mühlhäusser, *J. Prakt. Chem.* 1930, **125**, 211.
13 D. Coleman and A. C. Farthing, *J. Chem. Soc.* 1950, **0**, 3218.
14 R. Wilder and S. Mobashery, *J. Org. Chem.* 1992, **57**, 2755.
15 R. Katakai and Y. Iizuka, *J. Org. Chem.* 1985, **50**, 715.
16 H. Collet, C. Bied, L. Mion, J. Taillades and A. Commeyras, *Tetrahedron Lett.* 1996, **37**, 9043.
17 Y. Kamei, A. Sudo, H. Nishida, K. Kikukawa and T. Endo, *J. Polym. Sci., Part A-1: Polym. Chem.* 2008, **46**, 2525.
18 Y. Kamei, A. Nagai, A. Sudo, H. Nishida, K. Kikukawa and T. Endo, *J. Polym. Sci., Part A-1: Polym. Chem.* 2008, **46**, 2649.
19 Y. Kamei, A. Sudo, H. Nishida, K. Kikukawa and T. Endo, *Polym. Bull.* 2008, **60**, 625.
20 K. Koga, A. Sudo and T. Endo, *J. Polym. Sci., Part A-1: Polym. Chem.* 2010, **48**, 4351.
21 S. Guenes, H. Neugebauer and N. S. Sariciftci, *Chem. Rev.* 2007, **107**, 1324; A. Kraft, A. C. Grimsdale and A. B. Holmes, *Angew. Chem., Int. Ed.* 1998, **37**, 402; D. T. McQuade, A. E. Pullen and T. M. Swager, *Chem. Rev.* 2000, **100**, 2537.
22 K. M. Coakley and M. D. McGehee, *Chem. Mater.* 2004, **16**, 4533; J. Roncali, *Chem. Rev.* 1992, **92**, 711; J. M. Tour, *Chem. Rev.* 1996, **96**, 537.
23 M.-A. De Paoli, R. J. Waltman, A. F. Diaz and J. Bargon, *J. Polym. Sci., Polym. Chem. Ed.* 1985, **23**, 1687.
24 M. Leclerc and K. Faid, *Adv. Mater.* 1997, **9**, 1087.
25 R. D. McCullough, *Adv. Mater.* 1998, **10**, 93.
26 H. L. Wang, L. Toppare and J. E. Fernandez, *Macromolecules* 1990, **23**, 1053.
27 S. Alkan, L. Toppare, Y. Hepuzer and Y. Yagci, *J. Polym. Sci., Part A-1: Polym. Chem.* 1999, **37**, 4218.
28 A. Cirpan, S. Alkan, L. Toppare, I. Cianga and Y. Yagci, *J. Mater. Sci.* 2002, **37**, 1767.
29 J. D. Stenger-Smith, *Prog. Polym. Sci.* 1998, **23**, 57.
30 H. B. Yildiz, S. Kiralp, L. Toppare, Y. Yagci and K. Ito, *Mater. Chem. Phys.* 2006, **100**, 124.
31 E. Sahin, P. Camurlu, L. Toppare, V. M. Mercore, I. Cianga and Y. Yagci, *Polym. Int.* 2005, **54**, 1599.
32 E. Sahin, P. Camurlu, L. Toppare, V. M. Mercore, I. Cianga and Y Yagci, *J. Electroanal. Chem.* 2005, **579**, 189.
33 E. Unur, L. Toppare, Y. Yagci and F. Yilmaz, *Mater. Chem. Phys.* 2005, **91**, 261.
34 R. P. Kengne-Momo, F. Lagarde, P. Daniel, J. F. Pilard, M. J. Durand and G.Thouand, *Biointerphases* 2012, **7**, 67.
35 M. Lin, M. S. Cho, W. S. Choe and Y. Lee, *Biosens. Bioelectron.* 2009, **25**, 28.
36 D. Bhattacharyya and K. K. Gleason, *Chem. Mater.* 2011, **23**, 2600.
37 Y. Wen, D. Li, J. Xu, X. Wang and H. He, *Int. J. Polym. Mater.* 2013, **62**, 437.
38 S. Velayudham, C. H. Lee, M. Xie, D. Blair, N. Bauman, Y. K.Yap, S. A. Green and H. Liu, *ACS Appl. Mater. Interfaces* 2010, **2**, 104.
39 A. Sassolas, L. J. Blum, B. D. Leca-Bouvier, *Biotechnol. Adv.* 2012, **30,** 489.
40 Q. Gao, Y. Guo, J. Liu, X. Yuan, H. Qi, C. Zhang, *Bioelectrochemistry,* 2011, **81,** 109.
41 M. Tsai, Y. Tsai, *Sensor Actuat. B-Chem.* 2009, **141,** 592.
42 B. Demir, M. Seleci, D. Ag, S. Cevik, E. E. Yalcinkaya, D. O. Demirkol, U. Anik and S. Timur, *RSC Adv*. 2013, **3,** 7513.
43 C. Hea, J. Liua, Q. Zhanga, C. Wu, *Sensor Actuat. B-Chem.* 2012, **166,** 802.
44 A. Eftekhari, *Synth Metals.* 2004, **145**, 211.
45 R. Antiochia, L. Gorton, *Biosens. Bioelectron.* 2007, **22,** 2611.
46 T. Kong, Y. Chen, Y. Ye, K. Zhang, Z. Wang, X. Wang, *Sensor Actuat. B-Chem*. 2009, **138,** 344.
47 L. Su, X. Qiu, L. Guo, F. Zhang, C. Tung, *Sensor Actuat. B-Chem.* 2004, **99,** 499.
48 J. Zhang, C. Wang, S. Chen, D. Yuan, X. Zhong, *Enzyme Microb. Tech.* 2013, **52,** 134.
49 S. Cosnier, C. Gondran, A. Pellec, and A. Senillou, *Anal. Lett.* 2001, **34(1),** 61.
50 S. Demirci Uzun, N. Akbasoglu Unlu, M. Sendur, F. Ekiz Kanik, S. Timur, L. Toppare, *Colloid Surface B.* 2013, **112,** 74–80.
51 M. Kesik, F. Ekiz Kanik, G. Hızalan, D. Kozanoglu, E. Nalbant Esenturk, S. Timur, L. Toppare, *Polymer,* 2013, 54, 4463.

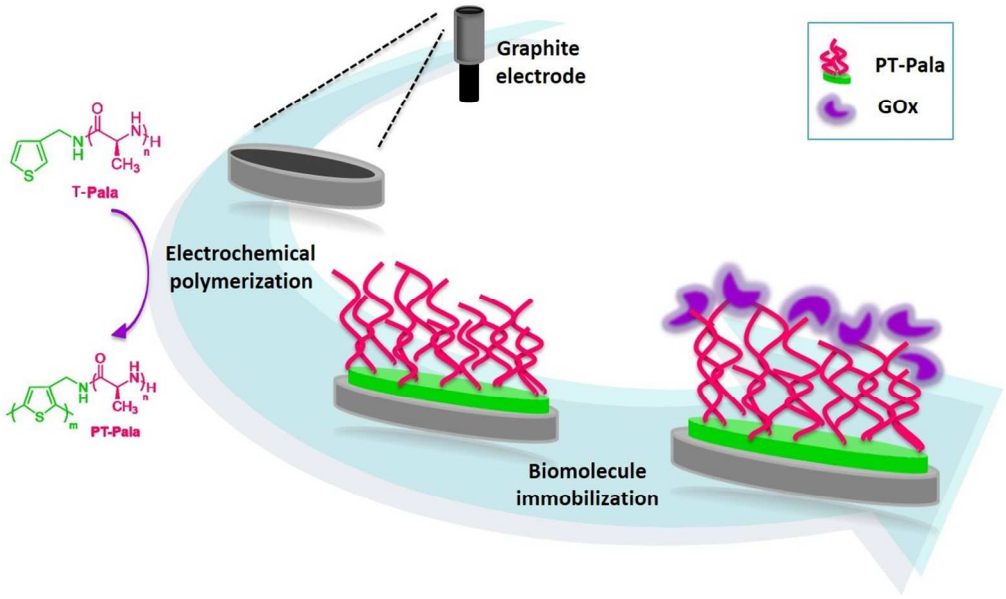

336x198mm (96 x 96 DPI)